

## Analysis of Supply Airflow Control by a Stratified Thermal Model in a VAV System

Seo Young Kim\*, Jeong Woo Moon\* and Hyung-Hee Cho\*\*

**Key words:** VAV system, Indoor air quality, Homogeneous lumped thermal model, Stratified thermal model, Supply airflow control, PI control

### Abstract

The present study concerns the numerical simulation of a supply airflow control in a variable air volume (VAV) system. A stratified thermal model (multi-zone model) is suggested to predict a local thermal response of an air-conditioned space. The effects of various thermal parameters such as the cooling system capacity, the thermal mass of an air-conditioned space, the time delay of thermal effect, and the building envelope heat transmission are investigated. Further, the influence of control parameters such as the supply air temperature, the PI control factor and the thermostat location on a VAV system is quantitatively delineated. The results obtained show that the previous homogeneous lumped thermal model (single zone model) may overestimate the time taken to the set point temperature. It is also found that there exist the appropriate ranges of the control parameters for the optimal airflow control of the VAV system.

### Nomenclature

<p><i>Bias</i> : fraction of airflow modulation when the temperature is at the set point</p> <p><i>Error</i> : difference between space temperature and set point temperature [°C]</p> <p><i>F<sub>0</sub></i> : nondimensional parameter, eq. (10)</p> <p><i>F<sub>02</sub></i> : nondimensional parameter, eq. (11)</p>	<p><math>(MC)_j</math> : mass-heat capacity at the <i>j</i>-th zone [J/°C]</p> <p><i>M</i> : number of zones</p> <p><i>min</i> : minimum airflow fraction</p> <p><i>n</i> : nondimensional time delay, eq. (13)</p> <p><i>PB</i> : proportional band of temperature [°C]</p> <p><i>PIF</i> : PI control parameter</p> <p><i>Q</i> : internal heat gain [W]</p> <p><i>R</i> : nondimensional parameter, eq. (12)</p> <p><i>t</i> : time [sec]</p> <p><i>t<sub>c</sub></i> : time constant in PI control [sec]</p> <p><i>T</i> : space temperature in the homogeneous lumped thermal model [°C]</p>
<p>* Thermal/Flow Control Center, Korea Institute of Science and Technology, P.O.Box 131, Cheongryang, Seoul 130-650, Korea</p> <p>** Department of Mechanical Engineering, Yonsei University, 134 Shinchondong, Seodaemoonku, Seoul 120-749, Korea</p>	

$T_e$	: outdoor temperature [°C]
$T_m$	: averaged space temperature [°C]
$T_s$	: set point temperature [°C]
$T_0$	: supply air temperature [°C]
$(UA)_j$	: heat transmittance from the building envelope at the $j$ -th zone [W/°C]
$(UA)_{j,j-1}$	: heat transmittance between the $j$ -th and the $(j-1)$ -th zones [W/°C]
$(UA)_{j+1,j}$	: heat transmittance between the $(j+1)$ -th and the $j$ -th zones [W/°C]
$V$	: volume flow rate of supply air [m <sup>3</sup> /sec]

### Greek symbols

$\rho c$	: heat capacity of supply air [J/m <sup>3</sup> °C]
$\theta$	: nondimensional temperature, eq. (9)

### Superscript

$i$	: time index
-----	--------------

### Subscripts

$j$	: zone index
$t - td$	: time delay prior to the current time

## 1. Introduction

With the recent development of civilization, peoples demand a comfortable environment for the working space in which they spend much more time than ever. For the reason, the air-conditioning of office rooms in modern buildings is indispensable to human comfort and health. In an attempt to obtain a high indoor air quality, many air conditioning methods have been developed so far. Among them, the VAV (variable air volume) system has been widely

used in the air-conditioning of modern office buildings.

The VAV system regulates the volume of supply air to compensate for varying load in a space. Advantages of the VAV system are a low initial cost, a low operating cost and a rapid response to a varying load. In spite of many advantages, however, the VAV system may not provide a comfortable environment until the system is properly operated. When the supply airflow is reduced down to 50–60 percent of maximum of a design volume flow according to the reduction in load, severe drafts may appear in the room.<sup>(1,2)</sup> Consequently, the indoor air quality of the air-conditioned space seriously deteriorates.

In an effort to overcome these problems, extensive research on the air movement in an air-conditioned space has been performed so far. Spitler et al.<sup>(3)</sup> performed experiments with varying inlet locations and sizes, inlet temperatures, and flow rates to provide the convective heat transfer coefficients for the building load simulation model. Jin and Qgilvie<sup>(4)</sup> experimentally investigated the effect of inlet configuration on the airflow patterns and the velocity distribution in a full-scale room. They reported that the flow pattern in the occupied zone was significantly changed by the inlet velocity and the inlet slot height and it was strongly nonlinear. Zhang et al.<sup>(5)</sup> studied the effects of the diffuser air velocities and internal heat loads on the flow characteristics. A perusal of the aforementioned works revealed that flow and thermal characteristics of an air-conditioned space nonlinearly depended on the size of the space and the time delay of delivery air.

In spite of nonlinearity of flow and thermal characteristics, however, it has been requested to build a linearized thermal model of an air-conditioned space for the optimal control strategy of an air-conditioning system. Zhang and Nelson<sup>(6)</sup> suggested a simple homogeneous lumped thermal model to numerically simulate

the flow and thermal response of an air-conditioned space by a supply airflow control. The thermal characteristic of an air-conditioned space was expressed by the time variation of a representative space temperature. Therefore, this model could not show the variation of local temperature in the air-conditioned space. In order to control the VAV system properly, however, the information for local temperatures of the space is required. For instance, the thermostats that provide input signal to a VAV controller are commonly located on the ceiling rather than on the side-wall due to the flexible interior structure of modern high-story buildings. The thermostat located on the ceiling may produce false temperature signals that are different from the temperature at the occupied zone. Consequently, human comfort at the occupied zone may not be fully achieved until the supply airflow control is implemented through the accurate prediction on local temperatures.

In the present study, therefore, we suggest a stratified thermal model (multi-zone model) to simulate the variation of local air temperature in an air-conditioned space, as shown in Fig. 1. The present study aims to obtain an optimal control scheme for a VAV system according to the various thermal and control parameters. The effects of thermal parameters such as the cooling system capacity, the thermal mass of air-conditioned space, the time delay of ther-

mal effect, and the building envelope heat transmission are investigated in detail. Further, the influence of control parameters, i.e., supply air temperature, the PI (proportional-integral) control factor and the thermostat location, on the VAV system is quantitatively delineated.

## 2. Modeling of air-conditioned space

In order to simulate the supply airflow control in a VAV system, Zhang and Nelson<sup>(6)</sup> suggested a homogenous lumped thermal model (single zone model) for an air-conditioned space:

$$(MC) \frac{dT}{dt} = (UA)(T_e - T) + Q - \rho c V (T - T_0) \quad (1)$$

where  $(MC)$  denotes the overall heat mass capacity and  $(UA)$  is the heat transmittance from the building envelope.  $Q$  is the internal heat gain in a space and  $V$  the volume flow rate. In the above homogeneous lumped thermal model, the temperatures of a space are expressed only as a representative space temperature,  $T$ . Consequently, this model can not predict the variation of local temperature in an air-conditioned space.

In an effort to simulate the variation of local temperature, the present study suggests the stratified thermal model as exhibited in Fig. 1. The stratified thermal model consists of multiple-zones divided according to the elevation of an air-conditioned space. Air supplied from the diffuser on the ceiling flows through the space from the upper zone to the lower zone, and eventually exhausts at the bottom. It is also assumed that there is no back flow and no internal heat gain in the space, and the heat transmission through the building envelope is constant at the respective zones. Thermophysical properties of air are assumed constant. Then, the stratified thermal model can be expressed as

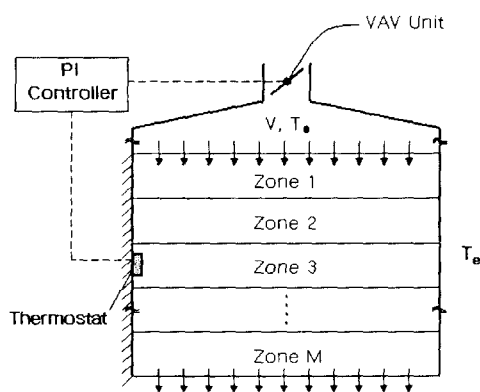


Fig. 1 Schematics of the stratified thermal model.

$$\begin{aligned}
(MC)_j \frac{dT_j}{dt} = & (UA)_j (T_e - T_j) \\
& - (UA)_{j,j-1} (T_j - T_{j-1}) \quad (2) \\
& + (UA)_{j+1,j} (T_{j+1} - T_j) \\
& - \rho c V (T_{j-1} - T_j) \\
& \text{for } j = 1, M
\end{aligned}$$

where,  $(MC)_j$  denotes the mass-heat capacity at the respective zones and  $(UA)_j$  is the heat transmittance from the building envelope. The  $(UA)_{j,j-1}$  and  $(UA)_{j+1,j}$  represent the heat transmittance between the proximity zones. The  $(UA)_{1,0}$  and  $(UA)_{M+1,M}$  at the end zones equal to zero.

A feedback control is widely adopted to maintain the set point temperature of the space. For the VAV system, the volume flow rate of supply air maintained at a constant temperature is changed according to the varying load. If the space temperature is different from the set point temperature, the VAV unit changes the volume flow rate of supply air through P (proportional) control or PI (proportional-integral) control according to the signal based on the temperature difference,  $T_j - T_s$ . The volume flow fraction of supply air  $x$  by the P control is defined as

$$x = \frac{(1 - \min)}{PB} \text{Error} + \text{Bias}, \quad \min \leq x \leq 1 \quad (3)$$

where  $PB$  denotes the proportional band of temperature,  $\min$  the minimum air flow fraction,  $\text{Bias}$  the fraction of airflow modulation when  $T_j = T_s$ , and  $\text{Error}$  the temperature difference:

$$\text{Error} = (T_j - T_s) \quad (4)$$

Here,  $T_j$  is the temperature at the  $j$ -th zone and  $T_s$  is the set point temperature of the

space. The volume flow rate of supply air in eq. (2) can be now expressed as

$$\begin{aligned}
V &= V_{\max} x \\
&= V_{\max} \left[ \frac{(1 - \min)}{PB} \text{Error} + \text{Bias} \right] \quad (5)
\end{aligned}$$

where  $V_{\max}$  is the maximum air flow rate of supply air in a VAV unit.

In a physical air conditioning system, the time delay may occur due to the time constant of a sensor, the actuating time of dampers, the delivery time of supply air to the space, and so forth. Considering these time delay effects, the eq. (3) is modified as follows.

$$\begin{aligned}
x &= \frac{(1 - \min)}{PB} (T_{j,t-td} - T_s) + \text{Bias}, \\
&\min \leq x \leq 1 \quad (6)
\end{aligned}$$

where  $T_{j,t-td}$  is the temperature of the  $j$ -th zone at a time delay  $td$  prior to the current time.

Generally, the P control has a disadvantage of the steady state offset<sup>(7)</sup> and may result in loss of control in a VAV unit. To solve this problem, the PI control is widely used. For PI control, the error in eq. (4) is modified as

$$\begin{aligned}
\text{Error} &= (T_{j,t-td} - T_s) \\
&+ \frac{1}{t_c} \int (T_{j,t-td} - T_s) dt \quad (7)
\end{aligned}$$

where  $t_c$  is a time constant. As  $t_c$  increases, the PI control becomes the P control. As  $t_c$  decreases, the PI control results in severe fluctuation of the system. Therefore, the time constant  $t_c$  in PI control should be properly selected at a value in-between.

Assume that  $(MC)_j$  and  $(UA)_j$  are constants, and  $(UA)_{j,j-1}$  equals to  $(UA)_{j+1,j}$ . Further, the temperatures at the respective

zones are assumed to be  $T_j < T_{j+1}$  for the cooling of the space. Then, the nondimensional equation of the stratified thermal model is:

$$\begin{aligned} \theta_j^i - \theta_{j-1}^{i-1} = & \\ & \frac{Fo_0}{n} [(\theta_e - \theta_{j-1}^{i-1}) - xR(\theta_j^{i-1} - \theta_{j-1}^{i-1})] \quad (8) \\ & + \frac{Fo_2}{n} (\theta_{j+1}^{i-1} - 2\theta_j^{i-1} + \theta_{j-1}^{i-1}) \end{aligned}$$

where,

$$\theta_j = \frac{(T_j - T_s)}{PB} \quad (9)$$

$$Fo_0 = \frac{(UA)_j}{(MC)_j} td \quad (10)$$

$$Fo_2 = \frac{(UA)_{j,j+1}}{(MC)_j} td \quad (11)$$

$$R = \frac{\rho c V_{\max}}{(UA)_j} \quad (12)$$

$$x = (1 - \min) \left[ \theta^{1-n} + PIF \Delta t \sum_{k=n}^i \theta^{k-n} \right], \quad (13)$$

$$\min \leq x \leq 1$$

$$n = \frac{td}{\Delta t} \quad (14)$$

Here,  $\Delta t$  is the time step for the numerical calculation and  $PIF$  in eq. (13) denotes the PI control factor.

### 3. Results and discussion

In the present study, the set point temperature, the initial temperature of the space, and the outdoor temperature were set at  $T_s = 19^\circ\text{C}$ ,  $T_j^0 = 25^\circ\text{C}$ , and  $T_o = 30^\circ\text{C}$ , respectively. The proportional band of temperature  $PB$  was set at  $25^\circ\text{C}$ . In the numerical calculation, the  $\Delta t$  was 1 sec and the time delay  $td$  was set at 36 sec.

First, the influence of the number of zone  $M$

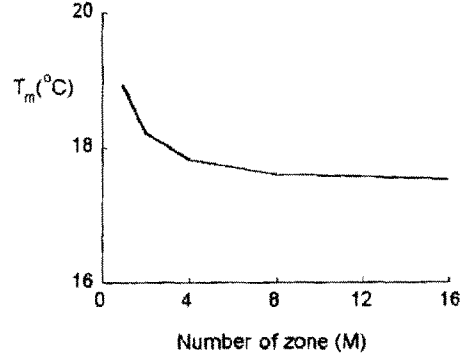
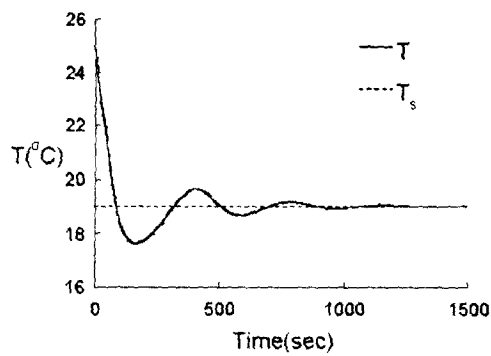
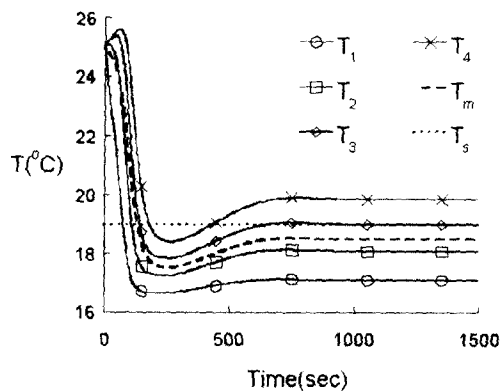


Fig. 2 Effect of number of zones on the steady state averaged space temperature.

on the averaged space temperature  $T_m$  at the steady state is investigated to determine the number of zone for the present simulation of the supply airflow control. Fig. 2 shows the variation of the averaged space temperature  $T_m$  according to the number of zone. Here, a cubic space of 2 m in height, 2 m in width, and 2 m in length was selected. The  $\rho c$  was  $1,228 \text{ J/m}^3\text{C}$ . The mass-heat capacity was set at  $(MC)_j = 2,519 \text{ J/C}$  and the heat transmittance from the building envelope was set at  $(UA)_j = 5.925 \text{ W/C}$  for the case of 4-zone simulation. The heat transmittance between the proximity zones in a space, i.e.,  $(UA)_{j,j-1}$  and  $(UA)_{j+1,j}$ , was  $0.208 \text{ W/C}$  when the mixed convection heat transfer coefficient in a conventional office room was considered.<sup>(8)</sup> As the number of zone increases, the averaged space temperature approaches an asymptotic value. For,  $M \geq 4$  the discrepancy in  $T_m$  is less than 1%. Therefore, four zones are selected for the entire simulation of supply airflow control in the present study.

Figure 3 demonstrates the discrepancy in the temporal variation of space temperatures between the previous homogeneous lumped thermal model<sup>(6)</sup> and the present stratified thermal model. For the previous lumped thermal model


 (a) Homogeneous lumped thermal model<sup>(6)</sup>


(b) Stratified thermal model

**Fig. 3** Comparison of temporal variation of the space temperature for two different thermal models.  $Fo=0.0883$ ,  $Fo_2=0.0008$ ,  $R=21.08$ ,  $\theta_0=-0.12$ , and  $PIF=0.05$ .

it is observed that the space temperature significantly fluctuates as seen in Fig. 3(a). However, the stratified thermal model in Fig. 3(b) displays a smooth variation of temperatures and results in a shorter time to the final steady state. This may be attributed to damping effects by heat transfer between the proximity zones. It should be noted that the temperature of the third zone  $T_3$  approaches the set point temperature  $T_s$  because the thermostat is located at the third zone. Therefore, the averaged space temperature  $T_m$  is shown slightly lower than the set point temperature.

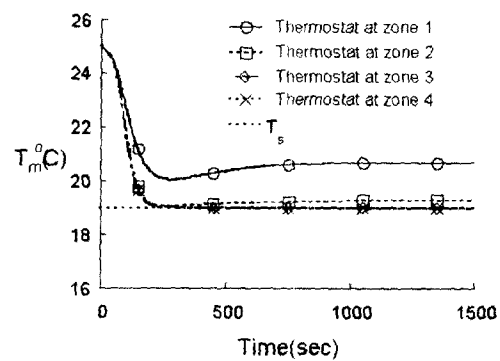


**Fig. 4** Effect of thermostat location on the averaged space temperatures.  $Fo=0.0883$ ,  $Fo_2=0.0008$ ,  $R=21.08$ ,  $\theta_0=-0.05$ , and  $PIF=0.05$ .

Figure 4 displays the effect of the thermostat location on the averaged space temperature. As a thermostat location moves down from the ceiling, the averaged space temperature  $T_m$  decreases to the set point temperature. Cold supply air induced at the ceiling eliminates the cooling load from the upper zone, i.e., the first zone. Therefore, the air at the upper zone is colder than that at the lower zone. This implies that the feedback control of a VAV unit based on the temperature signal detected from the thermostat located on the ceiling may result in a higher space temperature than the set point temperature. Consequently, the thermostat placed at a lower occupied zone is much preferable to human comfort.

The effect of heat transfer between the proximity zones  $Fo_2$  in the stratified thermal model is investigated in Fig. 5. When the  $Fo_2$  is small, i.e., heat transfer coefficients between the proximity zones are small, the space temperatures at the respective zones show a strong thermal stratification (Fig. 5(a)). As the  $Fo_2$  becomes large as displayed in Fig. 5(b), however, the space temperatures merge owing to the enhanced heat transfer between the proximity zones.

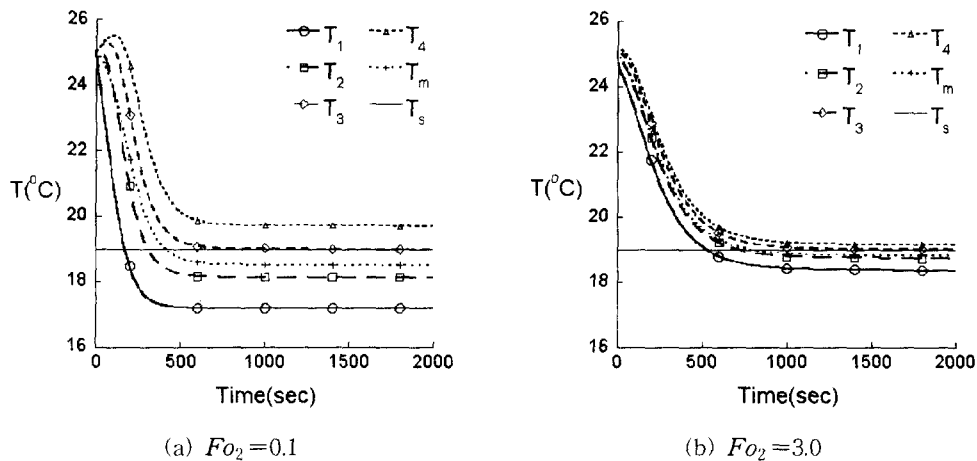


Fig. 5 Effect of  $Fo_2$  on the third zone temperature.  $Fo=0.05$ ,  $R=21.08$ ,  $\theta_0 = -0.12$ , and  $PIF=0.01$ .

The effect of  $Fo$  on the temporal variation of the third zone temperature  $T_3$  is shown in Fig. 6. The  $Fo$  is the nondimensional ratio of the time delay to the space time constant. Here, the space time constant is defined as the ratio of  $(MC)_j$  to  $(UA)_j$ . When the  $Fo$  is high, the averaged space temperature fluctuates significantly in the early stage. The high  $Fo$  is attributed to the high  $(UA)_j$  from the building envelope as well as to the small heat capacity  $(MC)_j$  of the air-conditioned space. Therefore, the air-conditioned space is significantly af-

ected by the change of the supply airflow. The time taken to the final steady state also increases as the  $Fo$  increases.

Figure 7 exhibits the effect of  $R$  on the temporal variation of the third zone temperature  $T_3$ . The  $R$  represents the nondimensional cooling capacity of the air-conditioning system compared to the effect of outdoor temperature. As the  $R$  increases, the space temperatures respond fast due to large cooling capacity of the air-conditioning system. Therefore, an air-conditioning system with a large cooling capacity cools down quickly the entire space.

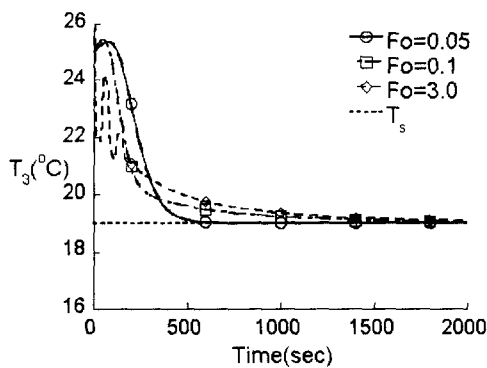


Fig. 6 Effect of  $Fo$  on the third zone temperature.  $Fo_2=0.0008$ ,  $R=21.08$ ,  $\theta_0 = -0.12$ , and  $PIF=0.01$ .

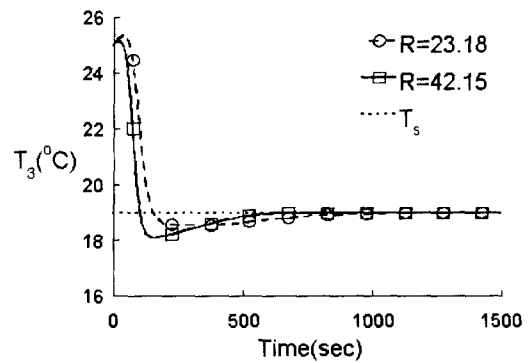


Fig. 7 Effect of  $R$  on the third zone temperature.  $Fo=0.0883$ ,  $Fo_2=0.0008$ ,  $\theta_0 = -0.08$ , and  $PIF=0.05$ .

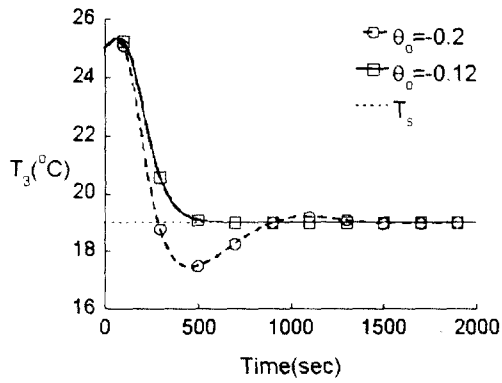


Fig. 8 Effect of  $\theta_0$  on the third zone temperature.  $Fo=0.05$ ,  $Fo_2=0.0008$ ,  $R=21.08$ , and  $PIF=0.01$ .

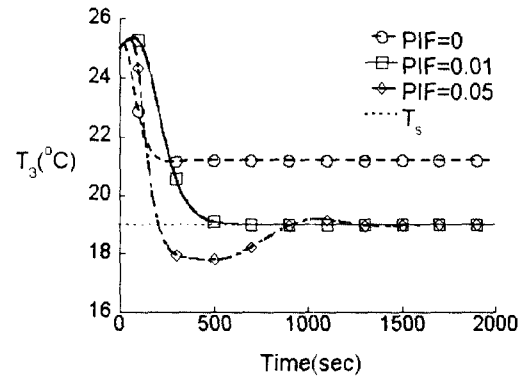


Fig. 9 Effect of  $PIF$  on the third zone temperature.  $Fo=0.05$ ,  $Fo_2=0.0008$ ,  $R=21.08$ , and  $\theta_0=-0.12$ .

However, the space may be much overcooled in the early stage when  $R$  is high.

The influence of the supply air temperature  $\theta_0$  on the third zone temperature  $T_3$  is de-

picted in Fig. 8. As the nondimensional temperature of supply air  $\theta_0$  decreases, much colder air is induced at the ceiling. As the absolute value of  $\theta_0$  increases, the space tem-

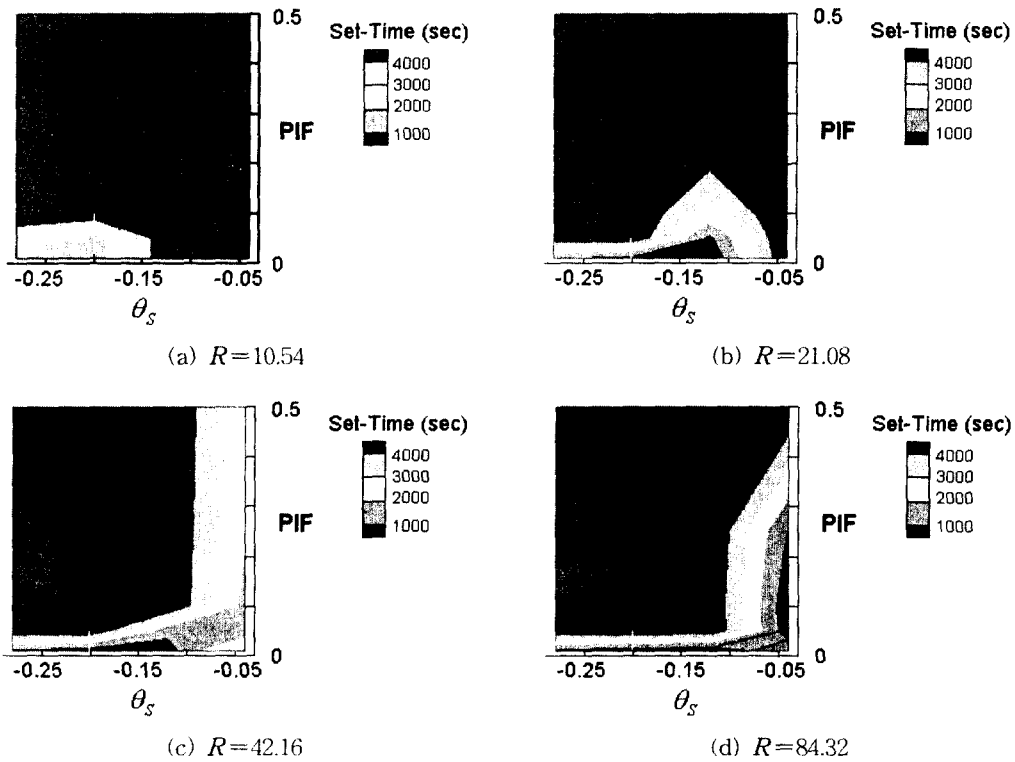


Fig. 10 Contour maps of the time taken to the set point temperature.  $Fo=0.05$  and  $Fo_2=0.0008$ .



perature becomes much sensitive to the variation of supply airflow. This results in an unstable response of the space temperature. When the absolute value of  $\theta_0$  is small, however, the space temperature shows a stable convergence to the set point temperature.

Figure 9 displays the effect of  $PIF$  parameter in the PI control scheme on the third zone temperature. When the  $PIF$  equals to zero, i.e., P control, the space temperature shows a steady state offset. As the  $PIF$  increases, however, the offset error disappears. When the high  $PIF$  value is selected ( $PIF=0.05$ ), the overcooling of the space occurs and the time to the final steady state is seriously delayed. It is caused by the overshoot in the term of the integral control in eq. (14).

By compiling numerical data, the contour maps for the optimal control of supply airflow

in a VAV unit according to the geometric parameters and the control parameters have been obtained. Fig. 10 shows the contour maps of the time taken to the final steady state. Here, the  $Fo$  is set to be small,  $Fo=0.05$ . When the  $R$  is small as displayed in Fig. 10 (a), the time to the steady state can be minimized at the region of a large  $|\theta_0|$  and a small  $PIF$ . As the  $R$  increases, however, the region for the minimum time is shifted to the region of an intermediate  $|\theta_0|$  and a small  $PIF$  (see Figs. 10 (b) and (c)). When the  $R$  is high as seen in Fig. 10 (d), the minimum time is achievable at the region of a small  $|\theta_0|$  and an intermediate  $PIF$  ( $0.05 < PIF < 0.25$ ).

As mentioned above, a small  $R$  denotes a small cooling capacity of an air-conditioning system for the cooling load in the space. In

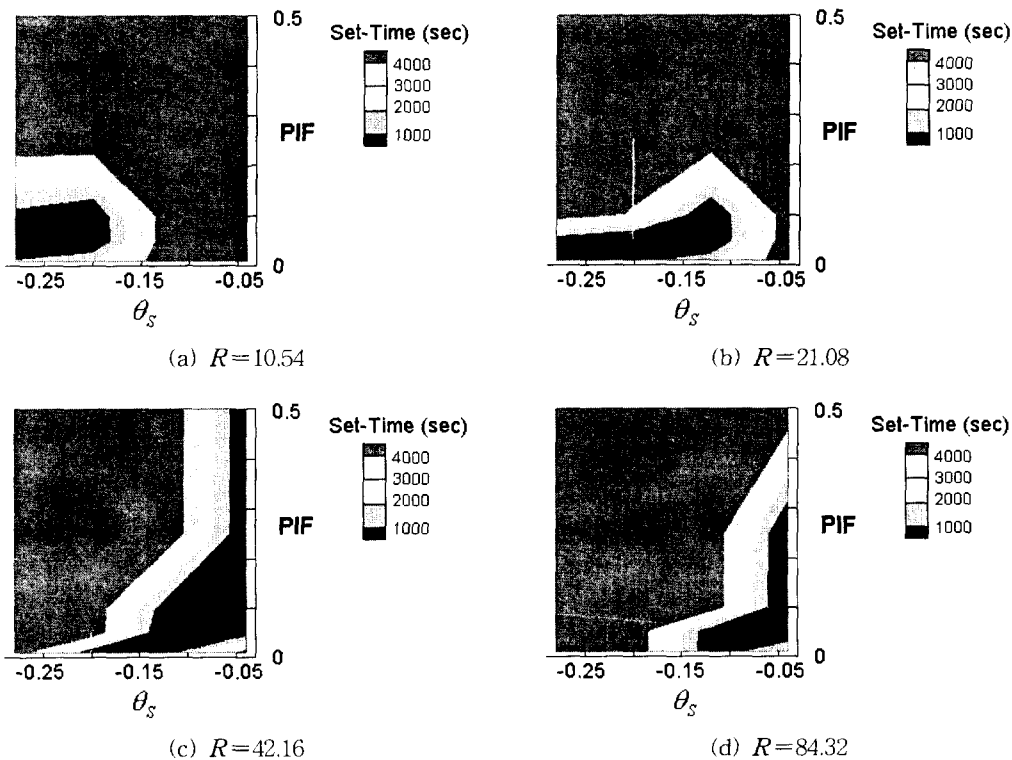


Fig. 11 Contour maps of the time taken to the set point temperature.  $Fo=0.5$  and  $Fo_2=0.0008$ .

order to get the set point temperature by a small  $R$  system, therefore, the supply air temperature should be low enough to overcome the cooling load. On the other hand, a high cooling capacity system of large  $R$  can obtain the set point temperature with a relatively warm supply air, i.e., a small  $|\theta_0|$ . For this case, even high  $PIF$  values can provide a stable convergence to the set point temperature.

When the  $Fo$  is large ( $Fo=0.5$ ), the effect of the supply air temperature  $|\theta_0|$  and the control parameter  $PIF$  on the time taken to the final steady state is exhibited in Fig. 11. The contour patterns are similar to those for  $Fo=0.05$ . However, the regions for optimal operation become wider compared to the case of a small  $Fo$ . A large  $Fo$  represents a small air-conditioned space when heat transmission from the building envelope is constant. Therefore, the air-conditioning system can handle the cooling load in the space at the wide ranges of supply air temperature and the  $PIF$  parameter. Consequently, it is necessary to select appropriate values for the control parameters in terms of the cooling capacity of the air-conditioning system, the cooling load and the size of the air-conditioned space.

#### 4. Conclusions

The simulation of supply airflow control in a variable air volume (VAV) system has been carried out. A stratified thermal model (multi-zone model) has been suggested to predict local thermal response of an air-conditioned space. The discrepancy between the present stratified thermal model and the previous homogeneous lumped thermal model (single-zone model) was described. For the stratified thermal model, the effects of various thermal parameters such as the cooling system capacity, the thermal mass of air-conditioned space, the time delay of ther-

mal effect, and the building envelope heat transmission were numerically investigated. Further, the influence of control parameters such as the supply air temperature, the PI control factor and the thermostat location on a VAV system was quantitatively delineated.

The simulation results show that the previous homogeneous lumped thermal model (single zone model) may overestimate the time taken to the set point temperature. It is also found that the appropriate ranges of the control parameters exist for the optimal control of the VAV system. For a small  $R$  system, much cold supply air with a small  $PIF$  value should be induced to eliminate the cooling load. As the  $R$  increases, the air-conditioning system can handle the cooling load with relatively warm supply air in the wide ranges of  $PIF$  values.

#### Acknowledgments

The present work was supported by a grant from the Energy Saving Project of the Ministry of Industry and Resources of Korea.

#### References

1. McQuiston, F. C. and Parker, J. D., 1994, Heating, Ventilating, and Air Conditioning Analysis and Design, 4th ed. John Wiley & Sons, Inc.
2. ASHRAE Handbook, 1996, Fundamentals of HVAC Control Systems, American Society of Heating, Refrigeration, and Air-conditioning Engineers.
3. Spitler, J. D., Pedersen, C. O. and Fisher, D. E., 1991, Interior convective heat transfer in buildings with large ventilative flow rates, ASHRAE Trans.: Symposia, Vol. 97, pp. 505-515.
4. Jin, Y. and Ogilvie, J. R., 1992, Isothermal airflow characteristics in a ventilated room with a slot inlet opening, ASHRAE Trans.: Symposia, Vol. 98, pp. 296-306.

5. Zhang, J. S., Wu, G. J. and Christianson, L. L., 1992, Full-scale experimental results on the mean and turbulent behavior of room ventilation flows, *ASHRAE Trans.: Symposia*, Vol. 98, pp. 307-318.
6. Zhang, Z. and Nelson, R. M., 1992, Parametric analysis of a building space conditioned by a VAV system, *ASHRAE Trans.: Research*, Vol. 98, pp. 43-48.
7. Ogata, K., 1990, *Modern Control Engineering*, 2nd ed., Prentice-Hall.
8. Mills, A. F., 1995, *Basic Heat and Mass Transfer*, 1st ed., Richard D. Irwin, Inc., pp. 274-279.